

How proper are Bayesian models in the astronomical literature?

Hyungsuk Tak,¹★ Sujit K. Ghosh,² and Justin A. Ellis³

¹*Department of Applied and Computational Mathematics and Statistics, University of Notre Dame, Notre Dame, IN 46556, USA*

²*Department of Statistics, North Carolina State University, Raleigh, NC 27695, USA*

³*Infinia ML, Durham, NC 27701, USA*

Accepted XXX. Received YYY; in original form ZZZ

ABSTRACT

The well-known Bayes theorem assumes that a posterior distribution is a probability distribution. However, the posterior distribution may no longer be a probability distribution if an improper prior distribution (non-probability measure) such as an unbounded uniform prior is used. Improper priors are often used in the astronomical literature to reflect a lack of prior knowledge, but checking whether the resulting posterior is a probability distribution is sometimes neglected. It turns out that 23 articles out of 75 articles (30.7%) published online in two renowned astronomy journals (*ApJ* and *MNRAS*) between Jan 1, 2017 and Oct 15, 2017 make use of Bayesian analyses without rigorously establishing posterior propriety. A disturbing aspect is that a Gibbs-type Markov chain Monte Carlo (MCMC) method can produce a seemingly reasonable posterior sample even when the posterior is not a probability distribution (Hobert and Casella 1996). In such cases, researchers may erroneously make probabilistic inferences without noticing that the MCMC sample is from a non-existing probability distribution. We review why checking posterior propriety is fundamental in Bayesian analyses, and discuss how to set up scientifically motivated proper priors.

Key words: Markov chain Monte Carlo (MCMC) – improper flat prior – vague prior – uniform prior – inverse gamma prior – non-informative prior – scientifically motivated prior

1 INTRODUCTION

A Bayesian model is uniquely determined by two components: (i) a likelihood function of unknown parameters θ given the data \mathbf{y} denoted by $L(\theta; \mathbf{y})$, which is proportional to a conditional probability density $f(\mathbf{y} | \theta)$ of a sampling distribution, and (ii) a joint prior density, $p(\theta)$. Using the fundamental Bayes theorem (see Appendix A for details), we can derive the posterior density of θ as follows¹:

$$\pi(\theta | \mathbf{y}) = \frac{f(\mathbf{y} | \theta)p(\theta)}{\int f(\mathbf{y} | \theta)p(\theta)d\theta} = \frac{L(\theta; \mathbf{y})p(\theta)}{\int L(\theta; \mathbf{y})p(\theta)d\theta}. \quad (1)$$

Even if the joint prior is improper (i.e., $\int p(\theta)d\theta = \infty$), the posterior density in Equation (1) can still be a valid probability density as long as the denominator is finite given the data \mathbf{y} , i.e., $\int L(\theta; \mathbf{y})p(\theta)d\theta < \infty$. The finite integrability

of the product $L(\theta; \mathbf{y})p(\theta)$ is called *posterior propriety*. It is often unnecessary to compute this integral because only a posterior kernel function, $q(\theta | \mathbf{y}) \equiv L(\theta; \mathbf{y})p(\theta)$, which is proportional to $\pi(\theta | \mathbf{y})$ if posterior propriety holds, is required to implement most MCMC algorithms.

Posterior propriety is crucial in MCMC, ensuring a couple of conditions for the convergence of a Markov chain. An irreducible, aperiodic, and recurrent Markov chain converges to a unique stationary distribution, and posterior propriety (with a random walk proposal) guarantees the aperiodicity and recurrence (p. 279, Gelman et al. 2013; Tierney 1994).

However, posterior propriety does not necessarily hold if the prior p is improper. For example, $\text{uniform}(0, \infty)$ and $\text{uniform}(-\infty, \infty)$ are widely used improper priors. Adopting such improper priors, one may fail to check posterior propriety because most MCMC methods do not require users to check posterior propriety, i.e., $\int L(\theta; \mathbf{y})p(\theta)d\theta < \infty$. When the posterior is improper, the most serious issue is that a Gibbs-type MCMC method may still appear to work well by producing a seemingly reasonable posterior sample from the path of the Markov chain (Hobert and Casella 1996). Consequently, researchers may continue making posterior

★ E-mail: hyungsuk.tak@gmail.com

¹ Within a finite-dimensional parametric framework, all density functions are formally defined with respect to a common dominating σ -finite measure like Lebesgue measure (or counting measure).

inferences without knowing that the MCMC sample is in fact drawn from a non-existent posterior probability distribution. [Hobert and Casella \(1996\)](#) first warned about this insidious feature of posterior impropriety. To prevent this, they recommended either proving posterior propriety (analytically) for improper priors or using jointly proper priors. Since then, statisticians have rigorously established posterior propriety using analytical techniques when improper priors are employed ([Daniels 1999](#); [Natarajan and Kass 2000](#); [Tak and Morris 2017](#)).

Posterior propriety is sometimes neglected in the astronomical literature. Our investigation reveals that 23 articles out of 75 (30.7%) published online in *ApJ* and *MNRAS* between Jan 1, 2017 and Oct 15, 2017 report Bayesian analyses without rigorously establishing posterior propriety. We hope that the posterior distributions of these 24 articles are actually proper, although it remains an open issue until posterior propriety is analytically established.

The rest of this article is organized as follows. Section 2 introduces a simple but non-trivial example of using an MCMC method for an improper posterior distribution. In Section 3, we investigate posterior propriety in 75 articles published online in *ApJ* and *MNRAS*. Section 4 discusses several ways to prove posterior propriety, focusing on using scientifically motivated proper priors which automatically guarantees posterior propriety.

2 A SIMPLE BUT NON-TRIVIAL EXAMPLE

Here we reproduce a classical example of [Hobert and Casella \(1996\)](#) that handles a Gaussian hierarchical model commonly used in Bayesian analyses. Suppose the observation y_j ($j = 1, \dots, n$) follows an independent Gaussian distribution given unknown mean μ_j with known measurement variance V_j . Also, μ_j follows another independent Gaussian distribution with unknown mean θ and unknown variance σ^2 :

$$y_j | \mu_j \sim N(\mu_j, V_j) \quad \text{and} \quad \mu_j | \theta, \sigma^2 \sim N(\theta, \sigma^2). \quad (2)$$

We set up a joint prior kernel function of θ and σ^2 as

$$p_1(\theta, \sigma^2) = p_1(\theta)p_1(\sigma^2) \propto \frac{1}{\sigma^2}, \quad (3)$$

which is improper because $\int_0^\infty \int_{-\infty}^\infty p_1(\theta, \sigma^2) d\theta d\sigma^2 = \infty$. The prior on σ^2 in Equation (3) is equivalent to both $d\sigma/\sigma$ and $d\log(\sigma)$, i.e., a widely used improper flat prior on a logarithmic scale of σ . The resulting posterior kernel function is

$$q(\boldsymbol{\mu}, \theta, \sigma^2 | \mathbf{y}) = p_1(\theta, \sigma^2) \prod_{j=1}^n \left[f(y_j | \mu_j) p(\mu_j | \theta, \sigma^2) \right], \quad (4)$$

where $\boldsymbol{\mu} = (\mu_1, \dots, \mu_n)$, $\mathbf{y} = (y_1, \dots, y_n)$, and density functions f and p are defined by Equation (2). This posterior kernel function is improper due to the prior on σ^2 regardless of the data; see Appendix B for a proof.

Although the posterior kernel function in Equation (4) is not a probability density, we can still derive its MCMC sampling scheme. Following [Hobert and Casella \(1996\)](#), we set $\mathbf{y} = (-10, 10)$, $n = 2$, and $V_j = 1$, but we keep using the notation V_j , y_j , and n for generality. We use a Gibbs

sampler ([Geman and Geman 1984](#)) that iteratively samples the following conditional posterior distributions: For $j = 1, 2$,

$$\begin{aligned} \mu_j | \boldsymbol{\mu}_{[-j]}, \theta, \sigma^2, \mathbf{y} &\sim N\left(\frac{\sigma^2 y_j + V_j \theta}{V_j + \sigma^2}, \frac{\sigma^2}{V_j + \sigma^2}\right), \\ \theta | \boldsymbol{\mu}, \sigma^2, \mathbf{y} &\sim N\left(\bar{\mu}, \frac{\sigma^2}{n}\right), \end{aligned} \quad (5)$$

$$\sigma^2 | \boldsymbol{\mu}, \theta, \mathbf{y} \sim \text{inverse-Gamma}\left(\frac{n}{2}, \frac{\sum_{j=1}^n (\mu_j - \theta)^2}{2}\right),$$

where $\boldsymbol{\mu}_{[-j]}$ denotes $\boldsymbol{\mu}$ without the j th component, $\bar{\mu}$ is the average of the elements of $\boldsymbol{\mu}$, and the inverse-Gamma(a, b) kernel function of x is $x^{-a-1} \exp(-b/x)$. At iteration i , for example, this Gibbs sampler updates each parameter in a sequence, i.e., $(\boldsymbol{\mu}^{(i)}, \theta^{(i-1)}, \sigma^{2(i-1)})$, $(\boldsymbol{\mu}^{(i)}, \theta^{(i)}, \sigma^{2(i-1)})$, and $(\boldsymbol{\mu}^{(i)}, \theta^{(i)}, \sigma^{2(i)})$. Almost all MCMC schemes for sampling multiple parameters use such Gibbs-type updates (either single-coordinate-wise or block-wise) at each iteration to form a Markov chain. We set the initial values as $\boldsymbol{\mu}^{(0)} = (-10, 10)$, $\theta^{(0)} = 0$, and $\sigma^{2(0)} = 1$, and draw 10,000 posterior samples of each parameter.

In Figure 1, we display the histogram, trace plot, and auto-correlation function of 10,000 posterior samples of θ on the top and those of $\log(\sigma^2)$ on the bottom. The posterior sample of θ concentrates on zero and that of $\log(\sigma^2)$ also forms a unimodal histogram. The trace plots show that the Markov chain explores the parameter space rapidly and the auto-correlation functions decrease quickly. The effective sample size² of θ is 8,140 and that of $\log(\sigma^2)$ is 1,847. Clearly, the Markov chain appears to converge to a certain probability distribution, and thus it makes sense to make a probabilistic inference using this posterior sample. However, if the initial value of σ^2 were close to zero at which the posterior kernel function puts infinite mass, the Markov chain would stay at $\sigma^2 = 0$ permanently without producing such a seemingly reasonable posterior sample. See [Hobert and Casella \(1996\)](#) for more theoretical details.

Such an inappropriate probabilistic inference based on a non-existing probability distribution can actually happen in reality unless posterior propriety is proven in advance. The article of [Pihajoki \(2017\)](#) published in *MNRAS* uses a similar but more complicated Gaussian hierarchical model that can be built upon a marginalized model of Equation (2), that is,

$$y_j | \theta, \sigma^2 \sim N(\theta, V_j + \sigma^2). \quad (6)$$

A model of [Pihajoki \(2017\)](#) replaces θ in Equation (6) with $\alpha + \beta x_j$, where α and β are unknown regression coefficients and x_j is some known covariate information with its known measurement variance V_{x_j} . Also, the model replaces V_j in Equation (6) with $\beta^2 V_{x_j} + V_j - 2\beta\rho(V_{x_j} V_j)^{0.5}$, multiplies σ^2 in Equation (6) by $1 + \beta^2$, and adopts an improper joint prior $d\alpha d\beta d\rho/d\sigma$; see Equations (33)–(37) of [Pihajoki \(2017\)](#).

² The effective sample size is defined as $n/(1+2\sum_{i=1}^{\infty}\rho(i))$, where n is the length of a Markov chain and $\rho(i)$ is the auto-correlation at lag i . The effective sample size becomes n if the sample from the path of a Markov chain is independent, i.e., $\rho(i) = 0$ for all i . We use a function `effectiveSize` of an R package `coda` ([Plummer et al. 2006](#)) to estimate the effective sample size.

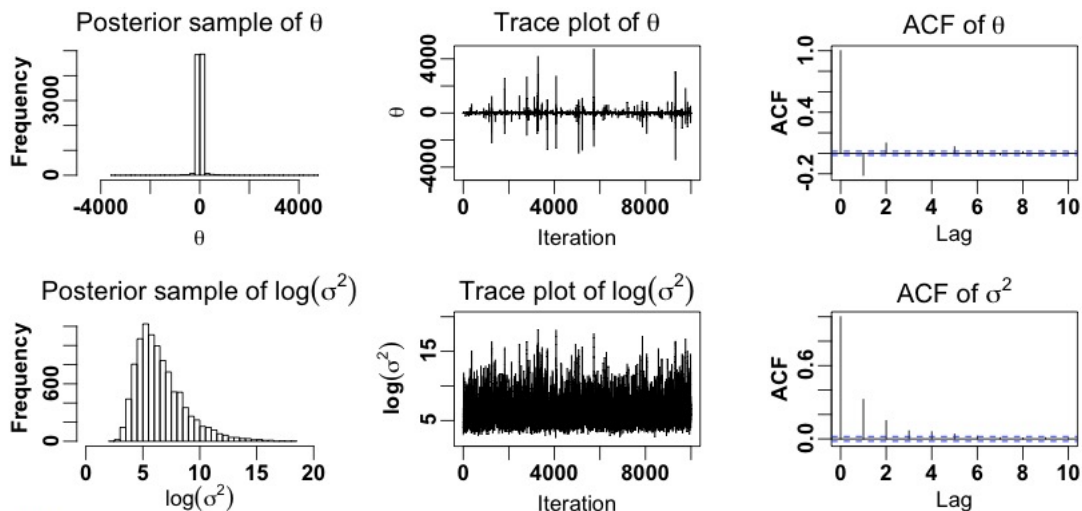


Figure 1. The result of sampling an improper posterior distribution in Equation (4). The histogram, trace plot, and auto-correlation function of 10,000 posterior samples of θ are on the top panels and those of $\log(\sigma^2)$ on the bottom panels. The Markov chain appears to converge to a certain probability distribution, although the target posterior distribution in Equation (4) is not a probability distribution.

This improper joint prior is equivalent to the problematic choice in Equation (3). The resulting posterior is not a probability distribution. This is because when $\beta = 0$, the model of Pihajoki (2017) becomes exactly the same as the one in Equation (6) that is improper with $d\text{ad}\sigma/\sigma$. Therefore, the integral of the posterior kernel function of Pihajoki (2017) is not finite.

The article of Pihajoki (2017) does not check posterior propriety before using an MCMC method. Thus, without recognizing posterior impropriety, the article makes a probabilistic inference using the seemingly reasonable posterior sample drawn from a non-existent posterior distribution. An MCMC method for this model may not show any evidence of posterior impropriety unless a Markov chain starts with the initial value of σ^2 close to zero. In practice, however, the inference in Pihajoki (2017) may be similar to that based on a proper posterior equipped with weakly informative proper priors. This is because it is likely that the Markov chain of Pihajoki (2017) resides in a safe (high-likelihood) region without exploring the entire parameter space.

One may think that we are exaggerating a problem with a pathological example where a tiny corner of the parameter space becomes a problem. We emphasize again that our concern is whether researchers are clearly aware that their Bayesian inferences are based on *probability distributions*. We have used such a tiny parameter space, e.g. $\sigma^2 \in [0, \epsilon)$ and $\beta = 0$, to raise a question about this concern, not to criticize Pihajoki (2017)'s omission in exploring this pathological region. Exploring the entire parameter space, however, is a useful practice to check a Markov chain's convergence. Inconsistent results from multiple Markov chains, whose initial values are spread across the parameter space, indicate the lack of convergence, e.g., due to multimodality or possibly posterior impropriety. A popular convergence diagnostic statistic of Gelman and Rubin (1992) is based on this idea. Initiating multiple Markov chains at least one of which begins near $\sigma^2 = 0$ might have indicated posterior impropriety in the case of Pihajoki (2017).

An astronomer's intuition or prior knowledge may in-

dicating which parameter space is scientifically meaningful to search a priori. This is invaluable information, but should be used carefully because one may have an incentive to initiate a Markov chain only in such a specific part of the parameter space. This chain might have stayed in that part, inevitably producing a result that is consistent with the astronomer's intuition. But, it is not desirable to report this result as if the entire parameter space were explored (even though a physically inspired model may have more power to constrain the region of interest than a non-physically inspired ones). Without being fully informed of such a limited search, readers may assume that evidence for multiple modes or posterior impropriety has not been found in the entire parameter space. Therefore, it is desirable to run multiple Markov chains with widely spread initial values across the parameter space or to use more tightly bounded priors to clarify which part is actually explored.

3 POSTERIOR PROPRIETY IN THE ASTRONOMICAL LITERATURE

We investigated the literature published online in *ApJ* and *MNRAS* between Jan 1, 2017 and Oct 15, 2017. On the webpages of IOPscience³ and *MNRAS*⁴, we found 75 articles whose titles or abstracts contain a word 'Bayesian'; see Appendix C for details of the selection. None of the 75 articles mention posterior propriety, and thus we checked further by classifying them into three categories; (a) priors are jointly proper; (b) priors are jointly improper; and (c) priors are not clearly specified. The last category includes cases where uniform (or flat) prior distributions are used without clearly specified ranges. Table 1 summarizes the classification; also see Appendix C for details. More than half of the articles use jointly proper priors. However, there are 23 articles in categories (b) and (c) that need proofs for posterior propriety

³ <http://iopscience.iop.org/>

⁴ <https://academic.oup.com/mnras>

Table 1. Classification of 75 articles published online in *ApJ* and *MNRAS* between Jan 1, 2017 and Oct 15, 2017 according to their prior distributions.

	<i>ApJ</i>	<i>MNRAS</i>
(a) Jointly proper priors	18	34
(b) Jointly improper priors	1	2
(c) Unclear priors	11	9
Total	30	45

to assure that their scientific arguments are actually based on proper posterior distributions.

The issue of the 20 articles in category (c) is not only posterior propriety but also reproducibility because their results cannot be reproduced without information about their priors. For instance, there are infinitely many uniform prior distributions according to their ranges, and thus a flat uniform prior is not a clear description. Proving posterior propriety can contribute to reproducible science as a by-product because its first step is to specify a Bayesian model clearly, i.e., a likelihood function of unknown parameters and their prior distributions.

Without hurting readability, one may be able to specify both likelihood function and priors in an appendix, mentioning only the resulting posterior propriety in the main text. This practice will greatly improve statistical clarity and reproducibility in the astronomical literature.

4 DISCUSSION

4.1 Proving posterior propriety

Improper prior distributions are widely used because they are mathematically convenient⁵ and are considered non-informative. A uniform $(-\infty, \infty)$ prior on a location parameter, e.g., $p_1(\theta)$ in Equation (3), is a Jeffreys' prior. It also has an advantage to make the data (likelihood function) speak more about the parameter when prior knowledge is limited, and results in a proper posterior distribution in many cases.

However, there is a cost to be paid for using improper priors, which is often neglected: *Proving posterior propriety*. Adopting an improper prior for even one parameter requires proving that the integral of a posterior kernel function over the entire parameter space is finite. It is challenging to develop a universal rule-of-thumb about when improper priors are likely to cause improper posterior and when they are not. This is because posterior propriety cannot be assured before it is actually proven on a case by case basis. The problematic choice $d\sigma^2/\sigma^2$ in Section 2, for example, does not cause posterior impropriety for a different Gaussian model such as $y_j | \mu, \sigma^2 \sim N(\mu, \sigma^2)$. With $p(\mu, \sigma^2) \propto 1/\sigma^2$, the resulting

⁵ We do not consider computational convenience including conjugacy because most astronomers are familiar with generic MCMC samplers, such as *PyStan* (Carpenter et al. 2017), *JAGS* (Denwood 2016), and *emcee* (Foreman-Mackey et al. 2013). These generic samplers automatically sample the target posterior given the likelihood and prior specifications, which enables choosing much wider classes of priors. *PyStan* and *JAGS* always require using proper priors, preventing potential posterior impropriety.

posterior is proper if $n \geq 2$; see Appendix D for a proof.

There are several ways to prove posterior propriety. The most rigorous one is to analytically show that the integral of the target posterior kernel function over the entire parameter space is finite. However, if the dimensions are large and the model is complicated, which is usually the case in the astronomical literature, it is challenging to prove posterior propriety analytically.

We can also apply existing theorems about posterior propriety only if a model considered in a theorem is the same as a candidate model to be used. For example, suppose a candidate model has two more parameters than a model whose posterior propriety is proven in a theorem. Posterior propriety of the candidate model holds if a marginalized candidate model (with the two additional parameters integrated out from the candidate model) is the same as the model considered in the theorem. This is because an unexpected term that is a function of unknown parameters may arise during the integration, which can make seemingly similar models completely different.

Jointly proper priors guarantee posterior propriety based on standard probability theory. Thus, when researchers want to adopt physically motivated improper priors whose posterior propriety is challenging to be proven, it is a useful practice to adopt proper priors that can mimic the behavior of the improper ones. The resulting posterior inference with mimicking proper priors will be almost identical to the one with improper priors. For a location parameter whose support is a real line, e.g., θ in Equation (3), a diffuse Gaussian or diffuse Student's t prior with an arbitrarily large scale can approximate an improper flat prior. The arbitrarily large scale of such a diffuse prior is a computational trick to approximate the improper flat prior although the scale itself may not make sense in practice. As for a parameter defined on a positive real line, e.g., σ^2 in Equation (3), a log-Normal, half Normal, and half Student's t with relatively large variance are known to be vague choices (Gelman 2006) that can approximate an improper flat prior $d\sigma^2$. Also, a uniform shrinkage prior, $d\sigma^2/(c + \sigma^2)^2$, where c is set to an arbitrarily large constant, can approximate $d\sigma^2$ with good frequentist coverage properties (Tak 2017).

4.2 Scientifically motivated proper priors for posterior propriety

Adopting scientifically motivated priors is one advantage of using Bayesian machinery because it provides a natural way to incorporate scientific knowledge into inference via priors. Proper priors are ideal for this purpose. Tak et al. (2017), for example, use a uniform $(-30, 30)$ prior for the unknown mean magnitude of a damped random walk process, considering a practical magnitude range from that of the Sun to that of the faintest object identifiable by the Hubble Space Telescope. This prior can be considered weakly informative because the range of the uniform prior is wide enough not to affect the resulting posterior inference. (A bounded uniform prior is not non-informative because its hard bounds completely exclude a certain range of parameter values.) If the range of a uniform prior is narrow and thus it significantly influences the posterior inference, such an informative choice may need further justification.

If one is uncomfortable about completely excluding a

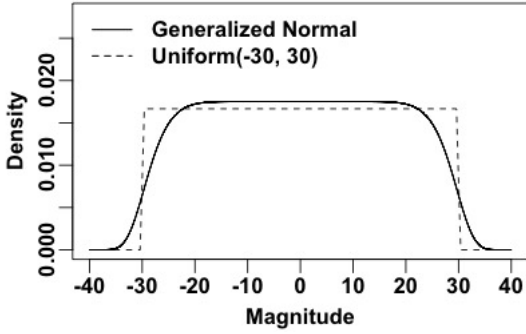


Figure 2. Prior distributions of magnitude. The density of the generalized Gaussian distribution with $\mu = 0$, $\sigma = 30$, and $s = 10$ is denoted by a solid curve and that of the uniform(-30, 30) distribution is represented by a dashed curve. As s increases, the two densities become close in shape. Unlike the uniform distribution whose hard bounds completely exclude a certain range of magnitude, the generalized Gaussian distribution sets up soft bounds.

certain parameter space, a generalized Gaussian distribution (Nadarajah 2005, 2006), also called a power exponential distribution, can be used to set up soft bounds. These soft bounds allow values outside the bounds with small but non-zero probability. Its kernel function of x is proportional to $\exp(-|(x - \mu)/\sigma|^s)$, where μ is the location parameter, σ is the scale parameter, and s is the shape parameter. The distribution approaches the uniform($\mu - \sigma, \mu + \sigma$) distribution, i.e., the tails of its density decrease more sharply, as s goes to infinity. Figure 2 displays its density function for $\mu = 0$, $\sigma = 30$, and arbitrarily chosen shape parameter $s = 10$ with the density of uniform(-30, 30) superimposed. A generalized Student's t distribution (McDonald and Newey 1988) can be an alternative if one prefers geometrically decreasing tails so that the data (likelihood) can dominate these bounds more easily (i.e., less informative).

For an unknown parameter whose support is the positive real line, an inverse-Gamma prior can be used as a scientifically motivated prior because it enables us to set up a soft lower bound of a parameter using scientific knowledge or past studies. The kernel function of x that follows an inverse-Gamma(a, b) distribution is $x^{-a-1} \exp(-b/x)$. Its mode, $b/(a + 1)$, plays a role of the soft lower bound, and a small shape parameter a is desirable for a weakly informative prior⁶. When x goes to infinity, the right tail of this kernel function decreases as a power law, while the left tail exponentially decreases as x approaches zero. Thus x is less likely to take on values much smaller than the mode (soft lower bound) a priori. See Figure 3 for a few density curves of inverse-Gamma(a, b) prior according to different values

⁶ An inverse-Gamma(a, b) prior is equivalent to an inverse- χ^2 prior with its degrees of freedom $2a$ and scale b/a . This relationship allows us to interpret the shape parameter of the inverse-Gamma as half the number of pseudo realizations that would carry equivalent information as the prior distribution. For example, an inverse-Gamma prior with the unit shape parameter, $a = 1$, carries a relatively small amount of information from two pseudo observations. If the number of observed data is much larger than two, the likelihood can dominate this inverse-Gamma prior with ease.

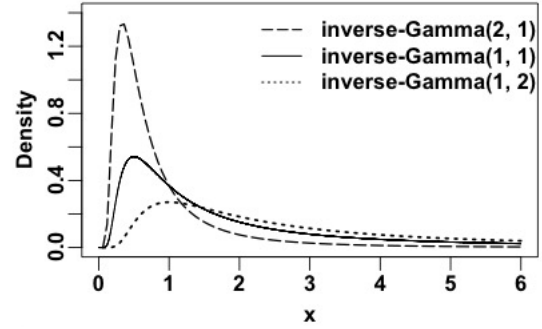


Figure 3. Three inverse-Gamma(a, b) densities according to different shape and scale parameters, a and b . We suggest using an inverse-Gamma(a, b) prior as a way to set up a soft lower bound of a random variable x a priori. The right tail geometrically decreases with power $a + 1$ and the left tail exponentially decreases, which indicates that x is less likely to take on values much smaller than the mode (soft lower bound), $b/(a + 1)$, a priori. A small value of the shape parameter is desirable for a weakly informative prior. Fixing the shape parameter first ($a \ll n$), we can adjust the scale parameter to set a scientifically motivated soft lower bound.

of a and b . Modeling quasar variability, for example, Tak et al. (2017) adopt an inverse-Gamma(1, b) prior for the unknown timescale (in days) of a damped random walk process. The scale parameter b is set to one day so that its soft lower bound, 0.5 day, is much smaller than any timescale estimates of 9,275 quasars in a past study (MacLeod et al. 2010) a priori.

For a second-level variance component in a Gaussian hierarchical model such as σ^2 in Equation (2), Gelman (2006) does not recommend an inverse-Gamma(a, b) prior with arbitrarily small values for both a and b as a non-informative choice⁷. This makes sense because an inverse-Gamma prior always sets up a soft lower bound a priori. When the likelihood puts significant weight at zero but with relatively small data size, it is difficult for the likelihood to dominate the soft lower bound that is located near zero. In this case, the resulting posterior inference becomes sensitive to the location of the soft lower bound. Thus when the data size is small, it is important to construct the soft lower bound carefully, considering scientific knowledge or past studies.

A multiply-broken power-law density, proposed by Professor Eric B. Ford during a personal communication, can be another easy-to-construct scientifically inspired prior for parameters defined on a positive real line. For example, a doubly-broken power-law density is defined as $p(x) \propto x^{-\alpha_1}$ for $0 < x \leq b_1$, $p(x) = \beta_2 x^{-\alpha_2}$ for $b_1 < x \leq b_2$, and $p(x) = \beta_3 x^{-\alpha_3}$ for $b_2 < x$. If $\beta_i = b_{i-1}^{\alpha_i - \alpha_{i-1}}$ for $i = 2, 3$, it becomes a smoothly broken power-law (e.g., Anchordoqui et al. 2014). Small values of powers, $\alpha_1 (< 1)$, α_2 , and $\alpha_3 (> 1)$, are desirable for weakly informative priors, and zero powers for α_1 and α_2 enable segment-wise uniform priors. All these parameters including the cut-offs b_1 and b_2 ($0 < b_1 < b_2$) need to reflect astronomical knowledge or past studies.

We summarize all these proper priors in Table 2.

⁷ The inverse-Gamma(a, b) density of σ^2 behaves similarly to $d\sigma^2/\sigma^2$ as a and b go to zero. However, a difference between two densities is that as σ^2 goes to zero, the former goes to zero, while the latter goes to infinity (possibly causing posterior impropriety).

Table 2. A few proper priors that can be set up easily to reflect scientific knowledge and past studies in a weakly informative way.

Distribution	Support	Kernel function	Note
uniform(a, b)	\mathbb{R}	$1/(b - a)$	Its hard bounds (a, b), where $a < b$ ($\in \mathbb{R}$), can reflect past studies.
generalized Gaussian	\mathbb{R}	$\exp(- (x - \mu)/\sigma ^s)$	μ ($\in \mathbb{R}$) is the location parameter, σ ($\in \mathbb{R}^+$) is the scale parameter, and s ($\in \mathbb{R}^+$) is the shape parameter. As $s \rightarrow \infty$, this distribution becomes uniform($\mu - \sigma, \mu + \sigma$), and thus ($\mu - \sigma, \mu + \sigma$) can be considered as soft bounds set to represent scientific knowledge. The choice of s may be arbitrary. A generalized t distribution can be an alternative whose tails decreases geometrically.
inverse-Gamma(a, b)	\mathbb{R}^+	$x^{-a-1} \exp(-b/x)$	a ($\in \mathbb{R}^+$) is the shape parameter and is treated as the amount of prior information. It is desirable to be small for a weakly informative prior ($a \ll n$). Given a , the scale parameter b ($\in \mathbb{R}^+$) is set to form a soft lower bound $b/(a + 1)$ that represent past studies.
multiply-broken power-law	\mathbb{R}^+	$x^{-\alpha_1} I_{(0 < x \leq b_1)} +$ $\beta_2 x^{-\alpha_2} I_{(b_1 < x \leq b_2)} +$ $\dots +$ $\beta_k x^{-\alpha_k} I_{(b_{k-1} < x)}$	Small values of powers, $\alpha_1, \dots, \alpha_k$, are desirable for a weakly informative prior. When $k = 1$, $\alpha_1 \in [0, 1)$ and $b_0 = 0$. If $k = 2$, $\alpha_1 \in [0, 1)$ and $\alpha_2 > 1$. For $k \geq 3$, $\alpha_1 \in [0, 1)$, $\alpha_j \geq 0$ for $j = 2, 3, \dots, k - 1$, and $\alpha_k > 1$. Segment-wise uniform priors are feasible if $\alpha_i = 0$ ($i \neq k$). If $\beta_i = b_{i-1}^{\alpha_i - \alpha_{i-1}}$ for $i \geq 2$, this power law becomes a continuous function. All powers and coefficients, α_i , b_i , and β_i , can reflect scientific knowledge.

4.3 Re-analysis of the example in Section 2 with jointly proper priors

Let us revisit the example in Section 2 to see an impact of adopting jointly proper priors. Instead of the improper choices in Equation (3), we set a diffuse Gaussian prior for θ and a weakly informative inverse-Gamma prior for σ^2 independently:

$$\theta \sim \mathcal{N}(0, 10^5) \text{ and } \sigma^2 \sim \text{inverse-Gamma}(10^{-2}, 1). \quad (7)$$

We first set the shape parameter of the inverse-Gamma(a, b) prior to 10^{-2} that is much smaller than the data size ($a \ll n$). Next we set $b = 1$ to construct a soft lower bound, 0.99, assuming that it reflects scientific knowledge a priori. We denote the joint prior distribution in Equation (7) by $p^*(\theta, \sigma^2)$. The resulting full posterior kernel function is

$$q^*(\boldsymbol{\mu}, \theta, \sigma^2 | \mathbf{y}) = p^*(\theta, \sigma^2) \prod_{j=1}^n \left[f(y_j | \mu_j) p(\mu_j | \theta, \sigma^2) \right], \quad (8)$$

where density functions f and p are defined in Equation (2). The corresponding Gibbs sampler updates each coordinate of $\boldsymbol{\mu}$ by its conditional posterior specified in Equation (5) but updates θ and σ^2 by

$$\begin{aligned} \theta | \boldsymbol{\mu}, \sigma^2, \mathbf{y} &\sim \mathcal{N} \left(\frac{(n/\sigma^2)\bar{\mu}}{n/\sigma^2 + 1/10^5}, \frac{1}{n/\sigma^2 + 1/10^5} \right), \\ \sigma^2 | \boldsymbol{\mu}, \theta, \mathbf{y} &\sim \text{inverse-Gamma} \left(\frac{n}{2} + \frac{1}{10^2}, \frac{\sum_{j=1}^n (\mu_j - \theta)^2}{n} + 1 \right). \end{aligned} \quad (9)$$

The conditional distribution of θ in Equation (9) is similar to that in Equation (5), considering that 10^{-5} is close to zero. The other simulation configuration is the same.

Figure 4 exhibits the sampling result. The ranges of the horizontal and vertical axes in each panel are the same as those of Figure 1 for a comparison. Because of the jointly proper priors in Equation (7), we know that the resulting posterior kernel function q^* in Equation (8) is proper and thus the posterior sample displayed in Figure 4 represents the target posterior distribution. Although not shown here,

the MCMC method produces nearly the same sampling result regardless of the initial value of σ^2 , meaning that the Markov chain converges no matter where it starts. The histogram of θ in Figure 4 has much shorter tails than that in Figure 1, although the histogram of $\log(\sigma^2)$ in Figure 4 is similar to that in Figure 1. The soft lower bound of $\log(\sigma^2)$, i.e., $\log(0.99) = -0.01$, is not close to the high density region. This indicates that the soft lower bound does not affect the resulting posterior inference even though there are just two data points; the degrees of freedom parameter of an equivalent inverse- χ^2 prior is 0.02. A sensitivity analysis, though not shown here, indicates that the results are robust as long as the scale parameter b of the inverse-Gamma($10^{-2}, b$) prior puts the soft lower bound on the left-hand side of the high-density region. The effective sample size improves greatly; it is 9,823 for θ and 2,668 for $\log(\sigma^2)$. Consequently, the inference on θ becomes quite different from that in Section 2, empirically showing that checking posterior propriety before using MCMC methods can make a significant difference.

4.4 Concluding remarks

It is well understood that any probabilistic tool such as Bayesian interface should be based on a probability distribution. Jointly proper priors lead to a proper posterior distribution and can be either vague or scientifically motivated. However, improper priors are sometimes used to represent the lack of prior knowledge. Such improper priors combined with a likelihood function can result in an improper posterior distribution that is not a probability measure. Therefore, when improper priors are adopted, posterior propriety must be carefully proven before using any MCMC methods, which can also improve statistical clarity and reproducibility. We hope that posterior propriety draws more attention when improper priors are used in the astronomical literature.

For a more complete Bayesian analysis, posterior propriety is not the only thing to be checked in practice. We list some procedures or practices essential for a good Bayesian analysis as the referee recommends. Above all, we

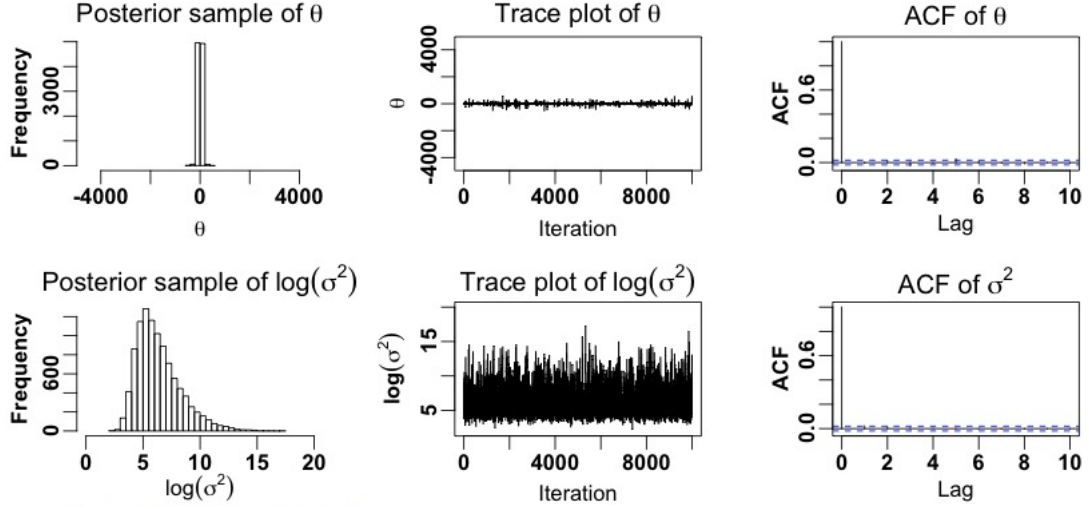


Figure 4. The result of sampling the proper posterior kernel function in Equation (8) that is based on weakly informative and vague proper priors in Equation (7). The histogram, trace plot, and auto-correlation function of 10,000 posterior samples of θ are on the top panels and those of $\log(\sigma^2)$ on the bottom panels. The ranges of vertical and horizontal axes are the same as those in Figure 1. Since priors in Equation (7) are jointly proper, we know that the resulting posterior q^* in Equation (8) is proper and thus the posterior sample is from q^* . Also, the sampling result hardly varies even if the initial value of σ^2 is close to zero. The ensuing Bayesian inference on θ is quite different from that in Section 2 with much shorter tails.

re-emphasize the importance of clarifying a Bayesian model, i.e., clearly specifying both likelihood function and priors, which is the beginning of the Bayesian analysis that precedes even checking posterior propriety. During the analysis, it is important to explore the entire (pre-specified) parameter space by implementing multiple Markov chains whose initial values are spread across the parameter space; it is desirable to specify the initial values of the chains. After the analysis, a good Bayesian analysis comes with various diagnostic procedures. An MCMC convergence check is necessary in both visual and numerical ways, e.g., trace plots, auto-correlation functions, effective sample sizes, and Gelman-Rubin diagnostic statistics (Gelman and Rubin 1992). As for model checking (Section 6, Gelman et al. 2013), a posterior predictive check is a valuable tool to assess a model’s consistency with the observed data, i.e., whether the model can explain the data generation process well. A prior predictive check (if priors are proper) is also useful for model checking, which generates a data set using a model with known parameter values and checks whether a fitted model can recover the generative parameter values. In addition, a sensitivity check is important to understand the influence of prior assumptions on the resulting posterior inference. We hope good Bayesian practice becomes more popular in the astronomical literature for more reliable Bayesian analysis.

ACKNOWLEDGEMENTS

Hyungsuk Tak and Sujit K. Ghosh acknowledge partial support from National Science Foundation grant DMS 1127914 (and DMS 1638521 only for Hyungsuk Tak) given to the Statistical and Applied Mathematical Sciences Institute. Justin A. Ellis acknowledges supports from the National Science Foundation Physics Frontier Center Grant 1430284 and from the National Aeronautics and Space Administration through Einstein Fellowship Grant PF4-150120. We thank David

E. Jones and David C. Stenning for a productive discussion at the International Centre for Theoretical Sciences in Bangalore, India, during a visit when participating in the program ‘Time Series Analysis for Synoptic Surveys and Gravitational Wave Astronomy’. We also thank Eric B. Ford for insightful comments, Christian P. Robert and Peter Coles for their discussions in their personal blogs, and the referee for invaluable suggestions.

APPENDIX A: THE BAYES THEOREM IN DETAIL

It is well known that a Bayesian statistical model consists of (i) a sampling distribution, $f(\mathbf{y} | \boldsymbol{\theta})$, denoting the conditional probability density of the data \mathbf{y} given unknown parameters $\boldsymbol{\theta}$; and (ii) a prior distribution, $p(\boldsymbol{\theta})$, denoting an unconditional probability density of $\boldsymbol{\theta}$. The resulting joint density of \mathbf{y} and $\boldsymbol{\theta}$ is $f(\mathbf{y} | \boldsymbol{\theta})p(\boldsymbol{\theta})$ based on standard probability theory. We can also express this joint density as a product of the unconditional density of the data $h(\mathbf{y}) \equiv \int f(\mathbf{y} | \boldsymbol{\theta})p(\boldsymbol{\theta})d\boldsymbol{\theta}$ and the so-called posterior density of $\boldsymbol{\theta}$ given \mathbf{y} , i.e.,

$$\pi(\boldsymbol{\theta} | \mathbf{y}) = \frac{f(\mathbf{y} | \boldsymbol{\theta})p(\boldsymbol{\theta})}{\int f(\mathbf{y} | \boldsymbol{\theta})p(\boldsymbol{\theta})d\boldsymbol{\theta}}. \quad (\text{A1})$$

All density functions are formally defined with respect to Lebesgue measure (or counting measure). However, in many scientific applications, we may relax the need for the use of a probability measure for the prior distribution by using a kernel function $k(\boldsymbol{\theta}) = c_0p(\boldsymbol{\theta})$ for some constant $c_0 > 0$ and also write the likelihood function $L(\boldsymbol{\theta}; \mathbf{y}) = c(\mathbf{y})f(\mathbf{y} | \boldsymbol{\theta})$ for some function $c(\mathbf{y}) > 0$. Then, as illustrated in Ghosh (2010), we can reexpress Equation (A1) as

$$\pi(\boldsymbol{\theta} | \mathbf{y}) = \frac{f(\mathbf{y} | \boldsymbol{\theta})p(\boldsymbol{\theta})}{\int f(\mathbf{y} | \boldsymbol{\theta})p(\boldsymbol{\theta})d\boldsymbol{\theta}} = \frac{L(\boldsymbol{\theta}; \mathbf{y})k(\boldsymbol{\theta})}{\int L(\boldsymbol{\theta}; \mathbf{y})k(\boldsymbol{\theta})d\boldsymbol{\theta}}. \quad (\text{A2})$$

As illustrated in Section 1, even if $\int k(\boldsymbol{\theta})d\boldsymbol{\theta} = \infty$, making the prior distribution improper, the posterior density as given in Equation (A2) is still a valid probability density as long as the denominator $\int L(\boldsymbol{\theta}; \mathbf{y})k(\boldsymbol{\theta})d\boldsymbol{\theta} < \infty$ is finitely integrable. However, an improper prior necessarily leads to improper marginal distribution of the data \mathbf{y} (and vice versa), i.e., $\int k(\boldsymbol{\theta})d\boldsymbol{\theta} = \infty$ is equivalent to $\int h(\mathbf{y})d\mathbf{y} = \infty$. This is because

$$\begin{aligned} \int h(\mathbf{y})d\mathbf{y} &= \int \int f(\mathbf{y} | \boldsymbol{\theta})p(\boldsymbol{\theta})d\boldsymbol{\theta} d\mathbf{y} \\ &= \int \int f(\mathbf{y} | \boldsymbol{\theta})p(\boldsymbol{\theta})d\mathbf{y} d\boldsymbol{\theta} = \int p(\boldsymbol{\theta})d\boldsymbol{\theta}, \end{aligned}$$

where the second equality holds from Fubini's theorem. This aspect is not a concern if $\pi(\boldsymbol{\theta} | \mathbf{y})$ is a proper probability density. It is well known that, in order to make an inference about $\boldsymbol{\theta}$ (or its function) conditional on the observed data, it is often sufficient to draw samples from a posterior kernel given by $L(\boldsymbol{\theta}; \mathbf{y})k(\boldsymbol{\theta})$, i.e., the numerator in Equation (A2) without the need to evaluate the denominator. Unfortunately, Gibbs-type MCMC methods can generate a sample from the posterior kernel which need not correspond to a proper posterior distribution; see [Hobert and Casella \(1996\)](#) for various examples. When a proper prior density $p(\boldsymbol{\theta})$ is used, this is not an issue as a posterior distribution is necessarily proper by standard probability theory. However, when an improper prior kernel is used, then the only option is to verify *analytically* that integral in the denominator of Equation (A2) is finite.

APPENDIX B: PROOF OF POSTERIOR IMPROPRIETY IN SECTION 2

The full posterior kernel function $q(\boldsymbol{\mu}, \theta, \sigma^2 | \mathbf{y})$ in Equation (4) is improper because the marginal posterior kernel function $q_1(\sigma^2 | \mathbf{y})$ with $\boldsymbol{\mu}$ and θ integrated out from $q(\boldsymbol{\mu}, \theta, \sigma^2 | \mathbf{y})$ is improper. We derive the marginal posterior kernel function of θ and σ^2 by integrating out $\boldsymbol{\mu}$ from $q(\boldsymbol{\mu}, \theta, \sigma^2 | \mathbf{y})$:

$$\begin{aligned} q_2(\theta, \sigma^2 | \mathbf{y}) &= \int_{\mathbb{R}^n} q(\boldsymbol{\mu}, \theta, \sigma^2 | \mathbf{y}) d\boldsymbol{\mu} \\ &= p_1(\theta, \sigma^2) \prod_{j=1}^n f_1(y_j | \theta, V_j + \sigma^2) \\ &= \frac{1}{\sigma^2} \exp\left(-\sum_{j=1}^n \frac{(y_j - \theta)^2}{2(V_j + \sigma^2)}\right) \prod_{j=1}^n (V_j + \sigma^2)^{-0.5} \\ &= \frac{1}{\sigma^2} \exp\left(-\sum_{j=1}^n \frac{(y_j - \hat{y})^2}{2(V_j + \sigma^2)} - \frac{(\theta - \hat{y})^2}{2V^*}\right) \prod_{j=1}^n (V_j + \sigma^2)^{-0.5}, \end{aligned} \tag{B1}$$

where density functions p_1 and f_1 are defined in Equations (3) and (6), respectively,

$$\hat{y} \equiv \frac{\sum_{j=1}^n y_j / (V_j + \sigma^2)}{\sum_{j=1}^n 1 / (V_j + \sigma^2)} \quad \text{and} \quad V^* \equiv \frac{1}{\sum_{j=1}^n 1 / (V_j + \sigma^2)}.$$

Next we marginalize out θ from Equation (B1) as follows:

$$\begin{aligned} q_1(\sigma^2 | \mathbf{y}) &= \int_{\mathbb{R}} q_2(\theta, \sigma^2 | \mathbf{y}) d\theta \\ &= \frac{(V^*)^{0.5}}{\sigma^2} \exp\left(-\sum_{j=1}^n \frac{(y_j - \hat{y})^2}{2(V_j + \sigma^2)}\right) \prod_{j=1}^n (V_j + \sigma^2)^{-0.5}. \end{aligned} \tag{B2}$$

This marginal posterior kernel function of σ^2 approaches infinity as σ^2 goes to zero due to the prior on σ^2 , i.e., $d\sigma^2/\sigma^2$. Therefore, $\int_{\mathbb{R}^+} q_1(\sigma^2 | \mathbf{y}) d\sigma^2 = \infty$.

APPENDIX C: CLASSIFICATION OF 75 ARTICLES IN SECTION 3

On the webpage of IOPscience, we found 33 *ApJ* articles whose titles or abstracts contain a word ‘Bayesian’. We excluded three of them because one is an erratum ([Eadie et al. 2017b](#)) and the other two use just Bayesian methods previously developed by other researchers ([Abeysekara et al. 2017](#); [Murphy et al. 2017](#)). We also obtained a list of 51 articles from the webpage of *MNRAS* that have the word ‘Bayesian’ in their abstracts. We did not consider six of them because one mentions a Bayesian analysis as a potential application ([Watkinson et al. 2017](#)), another uses a Bayesian information criterion for a model selection ([Wilkinson et al. 2017](#)), and the other four simply utilize Bayesian methods developed in other articles ([Pinamonti et al. 2017](#); [Green et al. 2017](#); [Sampedro et al. 2017](#); [Basak et al. 2017](#)).

Among the 30 articles published online in *ApJ*, 18 articles adopt jointly proper priors, and we classify these into category (a); [Fogarty et al. \(2017\)](#); [Montes-Solís and Arregui \(2017\)](#); [Zevin et al. \(2017\)](#); [Leung et al. \(2017\)](#); [Farnes et al. \(2017\)](#); [Benson et al. \(2017\)](#); [Sathyanarayana Rao et al. \(2017\)](#); [Sliwa et al. \(2017\)](#); [Park et al. \(2017\)](#); [Khrykin et al. \(2017\)](#); [Budavári et al. \(2017\)](#); [Wang et al. \(2017\)](#); [Scherrer and McKenzie \(2017\)](#); [Tabatabaei et al. \(2017\)](#); [Lund et al. \(2017\)](#); [Eadie et al. \(2017a\)](#); [Martínez-García et al. \(2017\)](#); [Küpper et al. \(2017\)](#).

[Knežević et al. \(2017\)](#) set an unbounded flat prior on the logarithm of the total flux without proving posterior propriety, and thus we classify this article into category (b).

We cannot check posterior propriety of 11 articles published online in *ApJ* because they do not specify priors clearly, i.e., their Bayesian models are not uniquely determined. We designate them as category (c) which contains cases where uniform (or flat) priors are used without clear ranges. Here we list them; [Kern et al. \(2017\)](#) use flat priors over the astrophysical parameters; [Bitsakis et al. \(2017\)](#) say nothing about priors; [Raithel et al. \(2017\)](#) do not specify a joint prior on five pressures; [Oyarzún et al. \(2017\)](#) utilize flat priors on all parameters; [Tanaka et al. \(2017\)](#) make use of uniform priors on m_{TRGB} and a ; [Mandel et al. \(2017\)](#) adopt a flat prior on μ_s whose range is unclear; [Daylan et al. \(2017\)](#) adopt uniform priors on many parameters; [Warren et al. \(2017\)](#) utilize an uninformative prior on β ; [Solá et al. \(2017\)](#) make use of an uninformative prior on h ; [Eilers et al. \(2017\)](#) do not specify priors on γ , σ_C , and σ_{ij} ; and [Jones et al. \(2017\)](#) use flat priors on SN Ia distances.

Next, we classify 45 articles published online in *MNRAS* into three categories. Category (a) contains 34 articles

whose priors are jointly proper; Ashton et al. (2017); Bainbridge and Webb (2017); Ata et al. (2017); Wagner-Kaiser et al. (2017); Cibirka et al. (2017); Patel et al. (2017); Si et al. (2017); Dwelly et al. (2017); Maund (2017); Davis et al. (2017); Hahn et al. (2017); Burgess (2017); Silburt and Rein (2017); MacDonald and Madhusudhan (2017); Abdurro'uf and Akiyama (2017); Kafle et al. (2017); Aigrain et al. (2017); Henderson et al. (2017); Kimura et al. (2017); Schellenberger and Reiprich (2017); Mejía-Narváez et al. (2017); Köhlinger et al. (2017); Dam et al. (2017); Garnett et al. (2017); Andrews et al. (2017); Kovalenko et al. (2017); McEwen et al. (2017); Oh et al. (2017); Duncan et al. (2017); Galvin et al. (2017); Salvato et al. (2017); Yu and Liu (2017); Greig and Mesinger (2017); and Sereno and Etori (2017)⁸.

Two articles published online in *MNRAS* employ improper priors without proving posterior propriety; Kos (2017) sets an improper prior on l_{se} without an upper limit; and we proved posterior impropriety of Pihajoki (2017) resulting from the improper prior on σ^2 .

We cannot judge posterior propriety of 9 articles published in *MNRAS* because their priors are not clearly specified; Rodrigues et al. (2017) adopt flat priors on metallicity and age; Vallisneri and van Haasteren (2017) do not specify priors on σ_{out} and c ; Binney and Wong (2017) use uniform priors for the logarithm of scale parameters; Ashworth et al. (2017) use flat priors on α_3 and A_V ; Jeffreson et al. (2017) utilize uniform priors on eight parameters (three are on the logarithmic scale); Molino et al. (2017) adopt flat priors on galaxy type and redshift; Accurso et al. (2017) do not specify priors on α and β_j ; Günther et al. (2017) adopt uniform priors on all parameters; and Igoshev and Popov (2017) do not clarify a joint prior on \vec{v}_o .

APPENDIX D: PROOF OF POSTERIOR PROPRIETY IN SECTION 4

The target posterior kernel function of μ and σ^2 is as follows:

$$\pi(\mu, \sigma^2 | \mathbf{y}) \propto (\sigma^2)^{n/2-1} \exp \left[-\frac{\sum_{i=1}^n (y_i - \mu)^2}{2\sigma^2} \right]. \quad (\text{D1})$$

⁸ In earlier preprints of this manuscript, we put their work into category (b). This is because Table 1 of Sereno and Etori (2017) sets `Z.max` = $+\infty$, resulting in an improper uniform prior on `mu.Z.0` whose upper limit is infinity. Specifically, the LIRA manual (Sereno 2017a) says, “`Z.max`: maximum value of the Z distribution. The Gaussian distribution and the prior on `mu.Z.0` are truncated above `Z.max`. If `n.mixture`>1, `Z.max` is automatically set to `n.large`.” Since the prior distribution on `mu.Z.0` is a uniform distribution as specified in Table 1 of Sereno and Etori (2017), its upper bound is infinity by specifying `Z.max` = $+\infty$. Although the prior on `mu.Z.0` is specified as an improper uniform prior in Table 1 of Sereno and Etori (2017), their code implementation is based on a bounded uniform prior on `mu.Z.0` (Sereno 2017a,b). Considering that their reported results are based on their code implementation with jointly proper prior distributions, we now put their work into category (a) despite the inconsistency between prior specification and code implementation. We hope that in the future the priors on both `Z` and `mu.Z.0` are separately specified with clear bounds of the uniform prior on `mu.Z.0` in a published article for a consistency between prior specification and code implementation.

The marginal posterior kernel function of σ^2 with μ integrated out from Equation (D1) is

$$\pi(\sigma^2 | \mathbf{y}) \propto (\sigma^2)^{-(n-1)/2-1} \exp \left[-\frac{\sum_{i=1}^n (y_i - \bar{y})^2}{2\sigma^2} \right]. \quad (\text{D2})$$

The integral of $\pi(\sigma^2 | \mathbf{y})$ in Equation (D2) is finite if n is greater than 1 because the marginal posterior distribution of σ^2 is inverse-Gamma($(n-1)/2$, $\sum_{i=1}^n (y_i - \bar{y})^2/2$), considering the functional form of $\pi(\sigma^2 | \mathbf{y})$ in Equation (D2).

REFERENCES

- Abdurro'uf and Akiyama, M. (2017). Understanding the Scatter in the Spatially Resolved Star Formation Main Sequence of Local Massive Spiral Galaxies. *Monthly Notices of the Royal Astronomical Society*, 469(3):2806–2820.
- Abeyssekara, A. U., Albert, A., Alfaro, R., Alvarez, C., Álvarez, J. D., Arceo, R., et al. (2017). Daily Monitoring of TeV Gamma-Ray Emission from Mrk 421, Mrk 501, and the Crab Nebula with HAWC. *The Astrophysical Journal*, 841(2):100.
- Accurso, G., Saintonge, A., Catinella, B., Cortese, L., Davé, R., Dunsheath, S. H., et al. (2017). Deriving a Multivariate α CO Conversion Function using the [CII]/CO (1–0) Ratio and its Application to Molecular Gas Scaling Relations. *Monthly Notices of the Royal Astronomical Society*, 470(4):4750–4766.
- Aigrain, S., Parviainen, H., Roberts, S., Reece, S., and Evans, T. (2017). Robust, Open-Source Removal of Systematics in Kepler Data. *Monthly Notices of the Royal Astronomical Society*, 471(1):759–769.
- Anchordoqui, L. A., Barger, V., Cholis, I., Goldberg, H., Hooper, D., Kusenko, A., et al. (2014). Cosmic Neutrino Pevatrons: A Brand New Pathway to Astronomy, Astrophysics, and Particle Physics. *Journal of High Energy Astrophysics*, 1–2:1–30.
- Andrews, J. J., Chanamé, J., and Agüeros, M. A. (2017). Wide Binaries in Tycho-Gaia: Search Method and the Distribution of Orbital Separations. *Monthly Notices of the Royal Astronomical Society*, 472(1):675–699.
- Ashton, G., Jones, D. I., and Prix, R. (2017). On the Free Precession Candidate PSR B1828–11: Evidence for Increasing Deformation. *Monthly Notices of the Royal Astronomical Society*, 467(1):164–178.
- Ashworth, G., Fumagalli, M., Krumholz, M. R., Adamo, A., Calzetti, D., Chandar, R., Cignoni, M., et al. (2017). Exploring the IMF of Star Clusters: A Joint SLUG and LEGUS Effort. *Monthly Notices of the Royal Astronomical Society*, 469(2):2464–2480.
- Ata, M., Kitaura, F.-S., Chuang, C.-H., Rodríguez-Torres, S., Angulo, R. E., Ferraro, S., et al. (2017). The Clustering of Galaxies in the Completed SDSS-III Baryon Oscillation Spectroscopic Survey: Cosmic Flows and Cosmic Web from Luminous Red Galaxies. *Monthly Notices of the Royal Astronomical Society*, 467(4):3993–4014.
- Bainbridge, M. B. and Webb, J. K. (2017). Artificial Intelligence Applied to the Automatic Analysis of Absorption Spectra. Objective Measurement of the Fine Structure Constant. *Monthly Notices of the Royal Astronomical Society*, 468(2):1639–1670.
- Basak, R., Iyyani, S., Chand, V., Chattopadhyay, T., Bhattacharya, D., Rao, A. R., and Vadawale, S. V. (2017). Surprise in Simplicity: An Unusual Spectral Evolution of a Single Pulse GRB 151006A. *Monthly Notices of the Royal Astronomical Society*, 472(1):891–903.
- Benson, B., Wittman, D. M., Golovich, N., Jee, M. J., van Weeren, R. J., and Dawson, W. A. (2017). MC 2 : A Deeper

- Look at ZwCl 2341.1+0000 with Bayesian Galaxy Clustering and Weak Lensing Analyses. *The Astrophysical Journal*, 841(1):7.
- Binney, J. and Wong, L. K. (2017). Modelling the Milky Way’s Globular Cluster System. *Monthly Notices of the Royal Astronomical Society*, 467(2):2446–2457.
- Bitsakis, T., Bonfini, P., González-Lópezlira, R. A., Ramírez-Siordia, V. H., Bruzual, G., Charlot, S., Maravelias, G., and Zaritsky, D. (2017). A Novel Method to Automatically Detect and Measure the Ages of Star Clusters in Nearby Galaxies: Application to the Large Magellanic Cloud. *The Astrophysical Journal*, 845(1):56.
- Budavári, T., Szalay, A. S., and Loredo, T. J. (2017). Faint Object Detection in Multi-Epoch Observations via Catalog Data Fusion. *The Astrophysical Journal*, 838(1):52.
- Burgess, J. M. (2017). The Rest-Frame Golenetskii Correlation via a Hierarchical Bayesian Analysis. *Monthly Notices of the Royal Astronomical Society*, page stx1159.
- Carpenter, B., Gelman, A., Hoffman, M. D., Lee, D., Goodrich, B., Betancourt, M., Brubaker, M. A., Guo, J., and Li, P. (2017). Rgbp: An R Package for Gaussian, Poisson, and Binomial Random Effects Models, with Frequency Coverage Evaluations. *Journal of Statistical Software*, 71(1):1–32.
- Cibirka, N., Cypriano, E. S., Brimiouille, F., Gruen, D., Erben, T., van Waerbeke, L., Miller, L., Finoguenov, A., Kirkpatrick, C., Henry, J. P., Rykoff, E., Rozo, E., Dupke, R., Kneib, J.-P., Shan, H., and Spinelli, P. (2017). CODEX Weak Lensing: Concentration of Galaxy Clusters at $z \sim 0.5$. *Monthly Notices of the Royal Astronomical Society*, 468(1):1092–1116.
- Dam, L. H., Heinesen, A., and Wiltshire, D. L. (2017). Apparent Cosmic Acceleration from Type Ia Supernovae. *Monthly Notices of the Royal Astronomical Society*, 472(1):835–851.
- Daniels, M. J. (1999). A Prior for the Variance in Hierarchical Models. *The Canadian Journal of Statistics*, 27(3):567–578.
- Davis, T. A., Bureau, M., Onishi, K., Cappellari, M., Iguchi, S., and Sarzi, M. (2017). WISDOM Project – II. Molecular Gas Measurement of the Supermassive Black Hole Mass in NGC 4697. *Monthly Notices of the Royal Astronomical Society*, 468(4):4675–4690.
- Daylan, T., Portillo, S. K. N., and Finkbeiner, D. P. (2017). Inference of Unresolved Point Sources at High Galactic Latitudes Using Probabilistic Catalogs. *The Astrophysical Journal*, 839(1):4.
- Denwood, M. J. (2016). runjags: An R Package Providing Interface Utilities, Model Templates, Parallel Computing Methods and Additional Distributions for MCMC Models in JAGS. *Journal of Statistical Software*, 71(9):1–25.
- Duncan, K. J., Brown, M. J. I., Williams, W. L., Best, P. N., Buat, V., Burgarella, D., et al. (2017). Photometric Redshifts for the Next Generation of Deep Radio Continuum Surveys - I: Template Fitting. *Monthly Notices of the Royal Astronomical Society*, page stx2536.
- Dwelly, T., Salvato, M., Merloni, A., Brusa, M., Buchner, J., Anderson, S. F., Boller, T., Brandt, W. N., et al. (2017). SPIDERS: Selection of Spectroscopic Targets Using AGN Candidates Detected in All-Sky X-ray Surveys. *Monthly Notices of the Royal Astronomical Society*, 469(1):1065–1095.
- Eadie, G. M., Springford, A., and Harris, W. E. (2017a). Bayesian Mass Estimates of the Milky Way: Including Measurement Uncertainties with Hierarchical Bayes. *The Astrophysical Journal*, 835(2):167.
- Eadie, G. M., Springford, A., and Harris, W. E. (2017b). Erratum: “Bayesian Mass Estimates of the Milky Way: Including Measurement Uncertainties with Hierarchical Bayes” (2017, ApJ, 835, 167). *The Astrophysical Journal*, 838(1):76.
- Eilers, A.-C., Hennawi, J. F., and Lee, K.-G. (2017). Joint Bayesian Estimation of Quasar Continua and the Ly α Forest Flux Probability Distribution Function. *The Astrophysical Journal*, 844(2):136.
- Farnes, J. S., Rudnick, L., Gaensler, B. M., Haverkorn, M., O’Sullivan, S. P., and Curran, S. J. (2017). Observed Faraday Effects in Damped Ly α Absorbers and Lyman Limit Systems: The Magnetized Environment of Galactic Building Blocks at Redshift = 2. *The Astrophysical Journal*, 841(2):67.
- Fogarty, K., Postman, M., Larson, R., Donahue, M., and Moustakas, J. (2017). The Relationship Between Brightest Cluster Galaxy Star Formation and the Intracluster Medium in CLASH. *The Astrophysical Journal*, 846(2):103.
- Foreman-Mackey, D., Hogg, D. W., Lang, D., and Goodman, J. (2013). emcee: The MCMC Hammer. *Publications of the Astronomical Society of the Pacific*, 125(925):306–312.
- Galvin, T. J., Seymour, N., Marvil, J., Filipović, M. D., Tothill, N. F. H., McDermid, R. M., et al. (2017). The Spectral Energy Distribution of Powerful Starburst Galaxies I: Modelling the Radio Continuum. *Monthly Notices of the Royal Astronomical Society*, page stx2613.
- Garnett, R., Ho, S., Bird, S., and Schneider, J. (2017). Detecting Damped Ly α Absorbers with Gaussian Processes. *Monthly Notices of the Royal Astronomical Society*, 472(2):1850–1865.
- Gelman, A. (2006). Prior Distributions for Variance Parameters in Hierarchical Models. *Bayesian Analysis*, 1(3):515–533.
- Gelman, A., Carlin, J. B., Stern, H. S., Dunson, D. B., Vehtari, A., and Rubin, D. B. (2013). *Bayesian Data Analysis*. CRC Press, Boca Raton, FL, USA.
- Gelman, A. and Rubin, D. B. (1992). Inference from iterative simulation using multiple sequences. *Statistical Science*, 7(4):457–472.
- Geman, S. and Geman, D. (1984). Stochastic Relaxation, Gibbs Distributions, and the Bayesian Restoration of Images. *IEEE Transactions on Pattern Analysis and Machine Intelligence*, (6):721–741.
- Ghosh, S. K. (2010). Basics of Bayesian Methods. In Bang, H., Zhou, X. K., van Epps, H. L., and Mazumdar, M., editors, *Statistical Methods in Molecular Biology*, pages 155–178. Humana Press, Totowa, NJ, USA.
- Green, J. A., Breen, S. L., Fuller, G. A., McClure-Griffiths, N. M., Ellingsen, S. P., Voronkov, M. A., Avison, A., et al. (2017). The 6-GHz Multibeam Maser Survey II. Statistical Analysis and Galactic Distribution of 6668-MHz Methanol Masers. *Monthly Notices of the Royal Astronomical Society*, 469(2):1383–1402.
- Greig, B. and Mesinger, A. (2017). Simultaneously Constraining the Astrophysics of Reionization and the Epoch of Heating with 21CMMC. *Monthly Notices of the Royal Astronomical Society*, 472:2651–2669.
- Günther, M. N., Queloz, D., Gillen, E., McCormac, J., Bayliss, D., Bouchy, F., et al. (2017). Centroid Vetting of Transiting Planet Candidates from the Next Generation Transit Survey. *Monthly Notices of the Royal Astronomical Society*, 472(1):295–307.
- Hahn, C., Vakili, M., Walsh, K., Hearin, A. P., Hogg, D. W., and Campbell, D. (2017). Approximate Bayesian Computation in Large-Scale Structure: Constraining the Galaxy–Halo Connection. *Monthly Notices of the Royal Astronomical Society*, 469(3):2791–2805.
- Henderson, C. S., Skemer, A. J., Morley, C. V., and Fortney, J. J. (2017). A New Statistical Method for Characterizing the Atmospheres of Extrasolar Planets. *Monthly Notices of the Royal Astronomical Society*, 470(4):4557–4563.
- Hobert, J. P. and Casella, G. (1996). The Effect of Improper Priors on Gibbs Sampling in Hierarchical Linear Mixed Models. *Journal of the American Statistical Association*, 91(436):1461–1473.
- Igoshev, A. P. and Popov, S. B. (2017). How to Make a Mature Accreting Magnetar. *Monthly Notices of the Royal Astronomical Society*, page stx2573.

- Jeffreson, S. M. R., Sanders, J. L., Evans, N. W., Williams, A. A., Gilmore, G. F., Bayo, A., et al. (2017). The Gaia-ESO Survey: Dynamical Models of Flattened, Rotating Globular Clusters. *Monthly Notices of the Royal Astronomical Society*, 469(4):4740–4762.
- Jones, D. O., Scolnic, D. M., Riess, A. G., Kessler, R., Rest, A., Kirshner, R. P., Berger, E., Ortega, C. A., Foley, R. J., Chornock, R., Challis, P. J., Burgett, W. S., Chambers, K. C., Draper, P. W., Flewelling, H., Huber, M. E., Kaiser, N., Kudritzki, R.-P., Metcalfe, N., Wainscoat, R. J., and Waters, C. (2017). Measuring the Properties of Dark Energy with Photometrically Classified Pan-STARRS Supernovae. I. Systematic Uncertainty from Core-collapse Supernova Contamination. *The Astrophysical Journal*, 843(1):6.
- Kafle, P. R., Sharma, S., Robotham, A. S. G., Pradhan, R. K., Guglielmo, M., Davies, L. J. M., and Driver, S. P. (2017). Galactic Googly: The Rotation–Metallicity Bias in the Inner Stellar Halo of the Milky Way. *Monthly Notices of the Royal Astronomical Society*, 470(3):2959–2971.
- Kern, N. S., Liu, A., Parsons, A. R., Mesinger, A., and Greig, B. (2017). Emulating Simulations of Cosmic Dawn for 21 cm Power Spectrum Constraints on Cosmology, Reionization, and X-Ray Heating. *The Astrophysical Journal*, 848(1):23.
- Khrykin, I. S., Hennawi, J. F., and McQuinn, M. (2017). The Thermal Proximity Effect: A New Probe of the He II Reionization History and Quasar Lifetime. *The Astrophysical Journal*, 838(2):96.
- Kimura, M., Kato, T., Isogai, K., Tak, H., Shidatsu, M., Itoh, H., et al. (2017). Rapid Optical Variations Correlated with X-rays in the 2015 Second Outburst of V404 Cygni (GS 2023+338). *Monthly Notices of the Royal Astronomical Society*, 471(1):373–382.
- Knežević, S., Läsker, R., van de Ven, G., Font, J., Raymond, J. C., Bailer-Jones, C. A. L., Beckman, J., Morlino, G., Ghavamian, P., Hughes, J. P., and Heng, K. (2017). Balmer Filaments in Tycho’s Supernova Remnant: An Interplay between Cosmic-ray and Broad-neutral Precursors. *The Astrophysical Journal*, 846(2):167.
- Köhlinger, F., Viola, M., Joachimi, B., Hoekstra, H., van Uitert, E., Hildebrandt, H., et al. (2017). KiDS-450: the Tomographic Weak Lensing Power Spectrum and Constraints on Cosmological Parameters. *Monthly Notices of the Royal Astronomical Society*, 471(4):4412–4435.
- Kos, J. (2017). Spatial Structure of Several Diffuse Interstellar Band Carriers. *Monthly Notices of the Royal Astronomical Society*, 468(4):4255–4272.
- Kovalenko, I. D., Stoica, R. S., and Emelyanov, N. V. (2017). Maximum a Posteriori Estimation Through Simulated Annealing for Binary Asteroid Orbit Determination. *Monthly Notices of the Royal Astronomical Society*, 471(4):4637–4647.
- Küpper, A. H. W., Johnston, K. V., Mieske, S., Collins, M. L. M., and Tollerud, E. J. (2017). Exploding Satellites—The Tidal Debris of the Ultra-faint Dwarf Galaxy Hercules. *The Astrophysical Journal*, 834(2):112.
- Leung, A. S., Acquaviva, V., Gawiser, E., Ciardullo, R., Komatsu, E., Malz, A. I., Zeimann, G. R., Bridge, J. S., Drory, N., Feldmeier, J. J., Finkelstein, S. L., Gebhardt, K., Gronwall, C., Hagen, A., Hill, G. J., and Schneider, D. P. (2017). Bayesian Redshift Classification of Emission-line Galaxies with Photometric Equivalent Widths. *The Astrophysical Journal*, 843(2):130.
- Lund, M. N., Aguirre, V. S., Davies, G. R., Chaplin, W. J., Christensen-Dalsgaard, J., Houdek, G., et al. (2017). Standing on the Shoulders of Dwarfs: The Kepler Asteroseismic LEGACY Sample. I. Oscillation Mode Parameters. *The Astrophysical Journal*, 835(2):172.
- MacDonald, R. J. and Madhusudhan, N. (2017). HD 209458b in New Light: Evidence of Nitrogen Chemistry, Patchy Clouds and Sub-Solar Water. *Monthly Notices of the Royal Astronomical Society*, 469(2):1979–1996.
- MacLeod, C., Ivezić, Ž., Kochanek, C., Kozłowski, S., Kelly, B., Bullock, E., Kimball, A., Sesar, B., Westman, D., Brooks, K., Gibson, R., Becker, A. C., and de Vries, W. H. (2010). Modeling the Time Variability of SDSS Stripe 82 Quasars as a Damped Random Walk. *The Astrophysical Journal*, 721(2):1014.
- Mandel, K. S., Scolnic, D. M., Shariff, H., Foley, R. J., and Kirshner, R. P. (2017). The Type Ia Supernova Color–Magnitude Relation and Host Galaxy Dust: A Simple Hierarchical Bayesian Model. *The Astrophysical Journal*, 842(2):93.
- Martínez-García, E. E., González-Lópezlira, R. A., Magris C., G., and Bruzual A., G. (2017). Removing Biases in Resolved Stellar Mass Maps of Galaxy Disks through Successive Bayesian Marginalization. *The Astrophysical Journal*, 835(1):93.
- Maund, J. R. (2017). The Resolved Stellar Populations Around 12 Type IIP Supernovae. *Monthly Notices of the Royal Astronomical Society*, 469(2):2202–2218.
- McDonald, J. B. and Newey, W. K. (1988). Partially Adaptive Estimation of Regression Models via the Generalized t Distribution. *Econometric Theory*, 4(3):428–457.
- McEwen, J. D., Feeney, S. M., Peiris, H. V., Wiaux, Y., Ringeval, C., and Bouchet, F. R. (2017). Wavelet-Bayesian Inference of Cosmic Strings Embedded in the Cosmic Microwave Background. *Monthly Notices of the Royal Astronomical Society*, 472(4):4081–4098.
- Mejía-Narváez, A., Bruzual, G., C., G. M., Alcaniz, J. S., Benítez, N., Carneiro, S., et al. (2017). Galaxy Properties from J-PAS Narrow-Band Photometry. *Monthly Notices of the Royal Astronomical Society*, 471(4):4722–4746.
- Molino, A., Benítez, N., Ascaso, B., Coe, D., Postman, M., Jovel, S., et al. (2017). CLASH: Accurate Photometric Redshifts with 14 HST Bands in Massive Galaxy Cluster Cores. *Monthly Notices of the Royal Astronomical Society*, 470(1):95–113.
- Montes-Solís, M. and Arregui, I. (2017). Comparison of Damping Mechanisms for Transverse Waves in Solar Coronal Loops. *The Astrophysical Journal*, 846(2):89.
- Murphy, K. D., Nowak, M. A., and Marshall, H. L. (2017). The Nuclear X-Ray Emission-line Structure in NGC 2992 Revealed by Chandra - HETGS. *The Astrophysical Journal*, 840(2):120.
- Nadarajah, S. (2005). A Generalized Normal Distribution. *Journal of Applied Statistics*, 32(7):685–694.
- Nadarajah, S. (2006). Acknowledgement of Priority: the Generalized Normal Distribution. *Journal of Applied Statistics*, 33(9):1031–1032.
- Natarajan, R. and Kass, R. E. (2000). Reference Bayesian Methods for Generalized Linear Mixed Models. *Journal of the American Statistical Association*, 95(449):227–237.
- Oh, S.-H., Staveley-Smith, L., Spekkens, K., Kamphuis, P., and Koribalski, B. S. (2017). 2D Bayesian Automated Tilted-Ring Fitting of Disk Galaxies in Large HI Galaxy Surveys: 2DBAT. *Monthly Notices of the Royal Astronomical Society*, page stx2304.
- Oyarzún, G. A., Blanc, G. A., González, V., Mateo, M., and III, J. I. B. (2017). A Comprehensive Study of Ly α Emission in the High-redshift Galaxy Population. *The Astrophysical Journal*, 843(2):133.
- Park, D., Barth, A. J., Woo, J.-H., Malkan, M. A., Treu, T., Benkert, V. N., Assef, R. J., and Pancoast, A. (2017). Extending the Calibration of C IV-based Single-epoch Black Hole Mass Estimators for Active Galactic Nuclei. *The Astrophysical Journal*, 839(2):93.
- Patel, E., Besla, G., and Mandel, K. (2017). Orbits of Massive Satellite Galaxies II. Bayesian Estimates of the Milky Way and Andromeda Masses Using High-Precision Astrometry and Cosmological Simulations. *Monthly Notices of the Royal As-*

- tronomical Society*, 468(3):3428–3449.
- Pihajoki, P. (2017). A Geometric Approach to Non-Linear Correlations with Intrinsic Scatter. *Monthly Notices of the Royal Astronomical Society*, 472(3):3407–3424.
- Pinamonti, M., Sozzetti, A., Bonomo, A. S., and Damasso, M. (2017). Searching for Planetary Signals in Doppler Time Series: A Performance Evaluation of Tools for Periodogram Analysis. *Monthly Notices of the Royal Astronomical Society*, 468(4):3775–3784.
- Plummer, M., Best, N., Cowles, K., and Vines, K. (2006). CODA: Convergence Diagnosis and Output Analysis for MCMC. *R News*, 6(1):7–11.
- Raithel, C. A., Özel, F., and Psaltis, D. (2017). From Neutron Star Observables to the Equation of State. II. Bayesian Inference of Equation of State Pressures. *The Astrophysical Journal*, 844(2):156.
- Rodrigues, T. S., Bossini, D., Miglio, A., Girardi, L., Montalbán, J., Noels, A., Trabucchi, M., Coelho, H. R., and Marigo, P. (2017). Determining Stellar Parameters of Asteroseismic Targets: Going Beyond the Use of Scaling Relations. *Monthly Notices of the Royal Astronomical Society*, 467(2):1433–1448.
- Salvato, M., Buchner, J., Budavári, T., Dwelly, T., Merloni, A., Brusa, M., Rau, A., Fotopoulou, S., and Nandra, K. (2017). Finding Counterparts for All-Sky X-Ray Surveys with Nway: A Bayesian Algorithm for Cross-Matching Multiple Catalogues. *Monthly Notices of the Royal Astronomical Society*, page stx2651.
- Sampedro, L., Dias, W. S., Alfaro, E. J., Monteiro, H., and Molino, A. (2017). A Multimembership Catalogue for 1876 Open Clusters Using UCAC4 Data. *Monthly Notices of the Royal Astronomical Society*, 470(4):3937–3945.
- Sathyanarayana Rao, M., Subrahmanyam, R., Shankar, N., and Chluba, J. (2017). Modeling the Radio Foreground for Detection of CMB Spectral Distortions from the Cosmic Dawn and the Epoch of Reionization. *The Astrophysical Journal*, 840(1):33.
- Schellenberger, G. and Reiprich, T. H. (2017). HICOSMO: Cosmology with a Complete Sample of Galaxy Clusters II. Cosmological Results. *Monthly Notices of the Royal Astronomical Society*, 471(2):1370–1389.
- Scherrer, B. and McKenzie, D. (2017). A Bayesian Approach to Period Searching in Solar Coronal Loops. *The Astrophysical Journal*, 837(1):24.
- Sereno, M. (2017a). *lira: Linear Regression in Astronomy*. R package version 2.0.0.
- Sereno, M. (2017b). The paper “How proper are Bayesian models in the astronomical literature?” [arXiv:1712.03549] by Tak, Ghosh and Ellis is improper. *arXiv 1712.05335*.
- Sereno, M. and Etori, S. (2017). CoMaLit-V. Mass Forecasting with Proxies: Method and Application to Weak Lensing Calibrated Samples. *Monthly Notices of the Royal Astronomical Society*, 468(3):3322–3341.
- Sí, S., van Dyk, D. A., von Hippel, T., Robinson, E., Webster, A., and Stenning, D. (2017). A Hierarchical Model for the Ages of Galactic Halo White Dwarfs. *Monthly Notices of the Royal Astronomical Society*, 468(4):4374–4388.
- Silburt, A. and Rein, H. (2017). Resonant Structure, Formation and Stability of the Planetary System HD155358. *Monthly Notices of the Royal Astronomical Society*, 469(4):4613–4619.
- Sliwa, K., Wilson, C. D., Matsushita, S., Peck, A. B., Petitpas, G. R., Saito, T., and Yun, M. (2017). Luminous Infrared Galaxies with the Submillimeter Array. V. Molecular Gas in Intermediate to Late-stage Mergers. *The Astrophysical Journal*, 840(1):8.
- Solá, J., Gómez-Valent, A., and de Cruz Pérez, J. (2017). First Evidence of Running Cosmic Vacuum: Challenging the Concordance Model. *The Astrophysical Journal*, 836(1):43.
- Tabatabaei, F. S., Schinnerer, E., Krause, M., Dumas, G., Meidt, S., Damas-Segovia, A., et al. (2017). The Radio Spectral Energy Distribution and Star-formation Rate Calibration in Galaxies. *The Astrophysical Journal*, 836(2):185.
- Tak, H. (2017). Frequency Coverage Properties of a Uniform Shrinkage Prior Distribution. *Journal of Statistical Computation and Simulation*, 87(15):2929–2939.
- Tak, H., Mandel, K., van Dyk, D. A., Kashyap, V. L., Meng, X.-L., and Siemiginowska, A. (2017). Bayesian Estimates of Astronomical Time Delays between Gravitationally Lensed Stochastic Light Curves. *The Annals of Applied Statistics*, 11(3):1309–1348.
- Tak, H. and Morris, C. N. (2017). Data-dependent Posterior Propriety of a Bayesian Beta-Binomial-Logit Model. *Bayesian Analysis*, 12(2):533–555.
- Tanaka, M., Chiba, M., and Komiyama, Y. (2017). Resolved Stellar Streams around NGC4631 from a Subaru/Hyper Suprime-Cam Survey. *The Astrophysical Journal*, 842(2):127.
- Tierney, L. (1994). Markov Chains for Exploring Posterior Distributions. *The Annals of Statistics*, 22(4):1701–1728.
- Vallisneri, M. and van Haasteren, R. (2017). Taming Outliers in Pulsar-Timing Data Sets with Hierarchical Likelihoods and Hamiltonian Sampling. *Monthly Notices of the Royal Astronomical Society*, 466(4):4954–4959.
- Wagner-Kaiser, R., Sarajedini, A., von Hippel, T., Stenning, D. C., van Dyk, D. A., Jeffery, E., Robinson, E., Stein, N., Anderson, J., and Jefferys, W. H. (2017). The ACS Survey of Galactic Globular Clusters XIV. Bayesian Single-Population Analysis of 69 Globular Clusters. *Monthly Notices of the Royal Astronomical Society*, 468(1):1038–1055.
- Wang, X., Jones, T. A., Treu, T., Morishita, T., Abramson, L. E., Brammer, G. B., et al. (2017). The Grism Lens-amplified Survey from Space (GLASS). X. Sub-kiloparsec Resolution Gas-phase Metallicity Maps at Cosmic Noon behind the Hubble Frontier Fields Cluster MACS1149.6+2223. *The Astrophysical Journal*, 837(1):89.
- Warren, H. P., Byers, J. M., and Crump, N. A. (2017). Sparse Bayesian Inference and the Temperature Structure of the Solar Corona. *The Astrophysical Journal*, 836(2):215.
- Watkinson, C. A., Majumdar, S., Pritchard, J. R., and Mondal, R. (2017). A Fast Estimator for the Bispectrum and Beyond - A Practical Method for Measuring Non-Gaussianity in 21-cm Maps. *Monthly Notices of the Royal Astronomical Society*, 472(2):2436–2446.
- Wilkinson, D. M., Maraston, C., Goddard, D., Thomas, D., and Parikh, T. (2017). firefly (Fitting Iteratively For Likelihood analysis): A Full Spectral Fitting Code. *Monthly Notices of the Royal Astronomical Society*, 472(4):4297–4326.
- Yu, M. and Liu, Q.-J. (2017). On the Detection Probability of Neutron Star Glitches. *Monthly Notices of the Royal Astronomical Society*, 468(3):3031–3041.
- Zevin, M., Pankow, C., Rodriguez, C. L., Sampson, L., Chase, E., Kalogera, V., and Rasio, F. A. (2017). Constraining Formation Models of Binary Black Holes with Gravitational-wave Observations. *The Astrophysical Journal*, 846(1):82.

This paper has been typeset from a $\text{\TeX}/\text{\LaTeX}$ file prepared by the author.